Fisheries New Zealand
Tini a Tangaroa

CCSBT-ERS/2203/12-A
(ERSWG Agenda item 5.1.3)

Hotspot analysis using Antipodean albatross as a test case

Part A: Assessing inter-annual variability in Antipodean albatross distributions in the Southern Hemisphere

Authors: Laura Tremblay-Boyer and Yvan Richard (Dragonfly Data Science)

Prepared for the 14th Meeting of the Ecologically Related Species Working Group (ERSWG14) of the Commission for the Conservation of Southern Bluefin Tuna (CCSBT)

March 2022

1. Introduction

Species distributions for seabirds can be difficult to quantify because individuals have an extensive range but use specific areas intensively. Also, area use changes over time and across breeding status. A previous assessment of the risk of surface longline fisheries for albatrosses and petrels in the Southern Hemisphere was presented to CCSBT ERSWG in 2019 (Abraham et al. 2019). This assessment developed distributions for all life stages of each of the 26 seabird taxa (including two sub-species for Antipodean albatross) from tracking data, following a methodology similar to that described by Carneiro et al (2020). Seabird distributions are particularly important in the application of spatial risk assessment approaches to inform management: seabird distributions and fishing effort data are combined to generate predictions of particular areas of high capture. Identification of these hotspots has been proposed as a tool for the spatial management of the surface-longline fishery in the CCSBT convention area.

Three limitations were raised following the analysis by Abraham et al. (2019) with regards to the development of seabird distributions from tracking data. First, tracking data were not available for all species, life stages and sites, so distribution data had to be augmented with pre-existing range maps lacking density information. Second, the generated distributions were static, i.e., all available tracking data were combined into a single distribution applied to all years. If seabird distributions vary between years, management relying on the average location of hotspots across years might not be effective. Finally, distributions derived purely from observations can be sensitive to individual bird behaviour, and high-use areas might be excluded by chance if none of the tracked individuals use them during tracking. This latter aspect is especially of concern for species for which little tracking data are available.

A key issue when attempting to address these limitations was the availability of tracking data for most seabird species. However, since then, there are now 158 000 locations that have been recorded for the Antipodean albatross sub-species *Diomedea antipodensis antipodensis*. In addition, previous work has already identified potential changes in the distribution of this species for some life-stages (Elliott & Walker 2017). Based on this data-rich tracking dataset, the Antipodean albatross is used here as a case study to explore some of the issues raised in the previous analysis. Temporal variability in distributions is re-assessed in light of tracking data availability throughout the time-series. As this project is ongoing, the current report summarises results to date and outlines expected future developments.

2. Methods

2.1 Input tracking data and grooming

All available tracking data for Antipodean albatross from 1997 onwards were acquired from the New Zealand Department of Conservation, with permission from private owners when applicable. We note that the 2019 risk assessment used an externally groomed version of this dataset (from the Birdlife International Seabird Tracking Database) but as recent tagging years are missing from this dataset from Antipodean albatross, grooming was redone on the original tracking data over the 1997–2021 period for internal consistency.

Tracking data were collected using PTT, GLS and GPS tracks over the 1997–2021 period. Geographical coordinates are directly available for PTT and GPS tags (either from the device itself for GPS tags or via the device provider for PTT tags). For GLS tags, locations

had to be estimated from the sunlight measurements and sea surface temperature recorded by the tracking device. The probGLS algorithm (Merkel et al. 2016) was used to generate a most-likely track from the median of the predicted locations for each observation. This approach estimates location with an error of less than 200km (Merkel et al. 2016) although precision changes throughout the year and is lower close to the equinoxes. Once a most-likely track was estimated for GLS tags, all locations for PTT, GLS and GPS tags were collated into a single dataset.

Life-history covariates were also available from the data provider, including the breeding status at the moment of tagging, sex and age of the individual. For analyses comparing adult distributions according to breeding status, individuals were classified as Breeders if their status was 'Breeder' or 'Nester', and Non-breeders if their status was 'Failed breeder', 'Failed nester', 'Non-breeder', 'Pre-breeder' or 'Bird On Ground (BOG)'.

Records of individual bird locations were groomed using the following set of rules:

- Records were removed if locations or dates were outside of latitudes -90 to 90 and time period 1997 to 2021;
- Records were removed if the individual speed from the previous location or to the next location (in km/hr, based on great circle distances) was in excess of 100 km/hr;
- Gaps of longer than 24 hours in the tracking data were discarded by splitting the deployment into separate segments;
- The first and/or last segments were removed if they contained less than 10 observations and were more than three months from the second and second-to-last segments respectively;
- Single segments were removed when they contained a single observation more than 1000km from previous or next segments;
- The start and/or end record within each segment were removed if their longitude or latitude were outside of the 0.5th to 99.5th quantile range for these values for the individual bird track, and if the speed to and from the record was in excess of 100 km/hr.

The groomed location records were then interpolated at regular time intervals of 30 minutes within each segment assuming linear displacement between records. No locations were interpolated between the separate segments. The interpolated records were assumed to reflect occupancy over the spatial range of the study. The first three days following deployment were removed to reduce a spatial bias caused by seabirds being tagged at the colony.

Following Abraham et al. (2019) and Carneiro et al. (2020), the gridded distributions were then generated by summing over all the interpolated records in each pixel of a pre-defined distribution grid. If needed, the density can be standardised so that all cells summed to 1. Distribution grids were defined at both the 1-degree resolution or at the 5-degree resolution. The latter matches the resolution of surface longline effort datasets and corresponds to the spatial resolution used in risk assessments. When applicable, records were first divided into categories (sex, breeding stage, year) before aggregation.

3.3 Estimation of the probability of cell inclusion in the distribution

A resampling approach was trialled to estimate the influence of tracking data availability on the size of the generated seabird distribution. The approach was implemented on female non-breeders, using only GPS tracks for consistency (n=25).

Individual tracks were randomly selected *n* times (without replacement) from the sample dataset and a distribution generated from this sub-sample. For this preliminary test, the resampling was repeated 100 times for track sample size (n) from 3 to 22. For each track sample size, the probability of cell inclusion in the final range was calculated from the proportion of times the cell was present in the distribution generated from each of 100 sub-samples. The high-probability area (in no. of cells) of the final range was calculated by summing the number of cells with a probability of inclusion greater than 0.95. The resampled areas were compared to the area of the distribution obtained when all 25 tracks were included in the estimated distribution.

3. Results

3.1 Characteristics of the input dataset

Following grooming, tracking data were available for Antipodean albatross for tags deployed between 1997 and 2001, 2003 and 2004, and 2011 to 2021 (Figure 1). The number of tags available was below 20 for all years up to 2019, after which it increased to over 60 in 2019 and 2020. There were only about 40 tags available for the last year of the study (2021) as some devices have yet to be recovered.

There were some changes in the tagging devices deployed over time: PTT devices were deployed exclusively up to 2004, then GLS devices between 2011 and 2018. GPS devices started being deployed in 2019, together with additional PTT devices (Figure 1, top panel).

Tags for both males and females are available for each year of the time-series, with a slightly higher proportion of females but no pronounced trend in the repartition (Figure 1, second panel). Tags were deployed almost exclusively on adults up to 2019, after which more than a third of deployed tags were on juveniles (except in 2021 but noting some tags are yet to be recovered) (Figure 1, third panel).

The distribution of breeding status has changed over time, with a higher proportion of breeders in earlier tagging years (Figure 1, bottom panel).

3.2 Preliminary trends in distributions by stage and over time

Estimated unstandardised distributions for Antipodean albatross (overall, for juveniles and for adults, by breeding status) are shown in Figures 2 to 8. The overall distribution highlights areas of higher use around the main colony of Antipodes Island and in surrounding waters, as well as around two distinct areas along the west coast of South America (Figure 2). The Tasman Sea also shows use by individuals but to a lesser extent. A coarser resolution

version of this map (from a 1- to 5-degree grid; Figure 3) shows the same trends with less precise delineation of high density hotspots (e.g. along the west coast of South America).

State-specific trends in spatial use emerge when the distributions are disaggregated by age and breeding status (Figures 4 to 8). Juveniles use waters eastward of the New Zealand North Island, as well as the Tasman Sea, extensively, but travel less far than adults (Figure 4). Female breeders utilise a restricted distribution centred on Antipodes Island but non-breeders forage across the Pacific, including in areas on the west coast of South America (Figures 5 and 6). Similarly, male breeders also foraged closer to Antipodes Island while the distribution of male non-breeders extended eastward including the west coast of South America (Figures 7 and 8). Male non-breeders appeared to use a wider latitudinal range than any of the other groups (Figure 8).

Time-series of distribution (grouped by observation year; Figures 9 to 12) capture the key spatial trends shown in the aggregated versions but with especially high inter-annual variability in low sample years.

3.3 Influence of tracking data availability on distribution size

A resampling approach was trialled to assess the influence of sample size on estimated distributions, using GPS tracks for female non-breeders. There are 25 tracks available for this subset, spanning 2019 and 2020, with observed positions ranging from the Tasman Sea to the Eastern Pacific (Figure 13).

Distributions were generated from 100 random subsets of these tracks (see Figure 14 as an example). As the number of tracks sampled increased from 3 to 10, the core range (defined here as the area where cells were included in more than 95% of the samples) expanded from the area eastward of Antipodes Island to the west coast of South America (Figure 15). When 20 tracks (i.e. 80% of the full dataset) were included in the sample, additional cells in upper or lower latitudes were included with higher probability. The area of the core range increased fastest from subsamples of 3 to 10 tracks, then at a slower rate thereafter (Figure 16). The longitudinal range was mapped with higher probability at lower sample sizes than the latitudinal range, indicating that fewer individuals utilise higher or lower latitudinal bands compared to the core longitudinal area such that a higher sample size might be required to characterise it (Figure 15).

4. Conclusion

This preliminary analysis confirmed key spatial differences in the distribution of Antipodean albatross by breeding status, age and sex, and further delineates the distribution of juvenile birds. A proposed resampling approach applied to non-breeder female GPS tags confirmed that low track sample sizes can influence key features of the estimated species distribution, such as the extent. This approach will be expanded to include other features of the distribution, e.g. the distribution of high-density areas (‘hotspots’), and test temporal variability in distributions by breeding stage for the 1997 to 2021 time-period. Of note, there are still features in the tagging dataset that are being explored, such as the optimal way to

assign breeding status from the breeding status at tagging, especially for tracks that extend in duration beyond 1 year. This stems from the observation of some tracks by breeding birds extending to the west coast of South America, which appears unlikely given the travel time needed from the colony. The plausibility of individual records north of the 25th parallel S are also being investigated.

Advantages of a resampling approach to analyse spatial features in the tracking dataset include the identification of track sample size thresholds below which the generated distributions are unlikely to be representative. Probability distributions for metrics of interest (e.g. the probability of cell inclusion in the distribution) could also be propagated to other components of a risk assessment analysis (e.g. hotspot delineation, capture estimates, etc.).

Figures

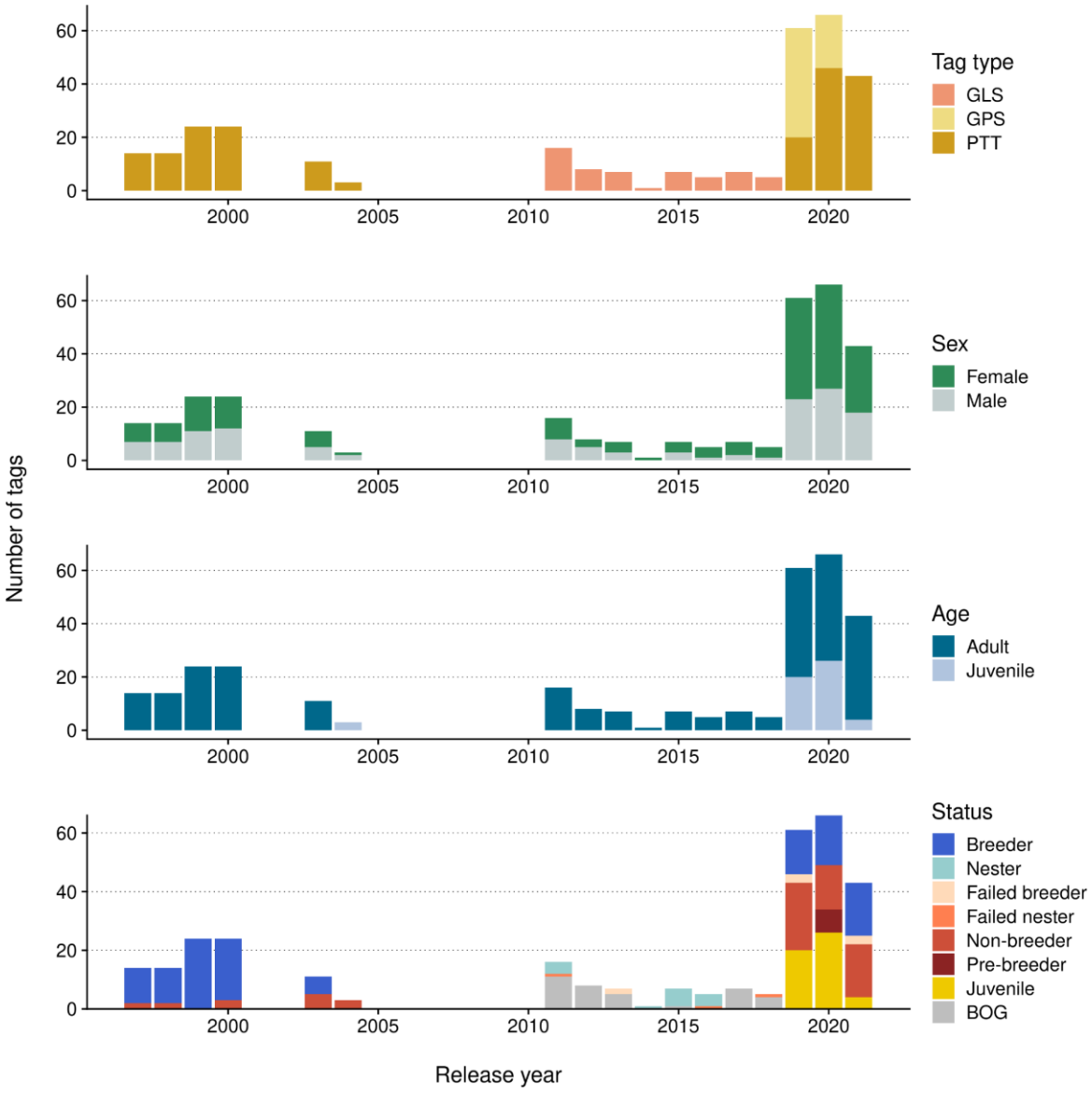

Figure 1: Description of groomed tracking dataset by tagging device type, individual sex, age and breeding status at tagging (BOG=Bird On Ground).

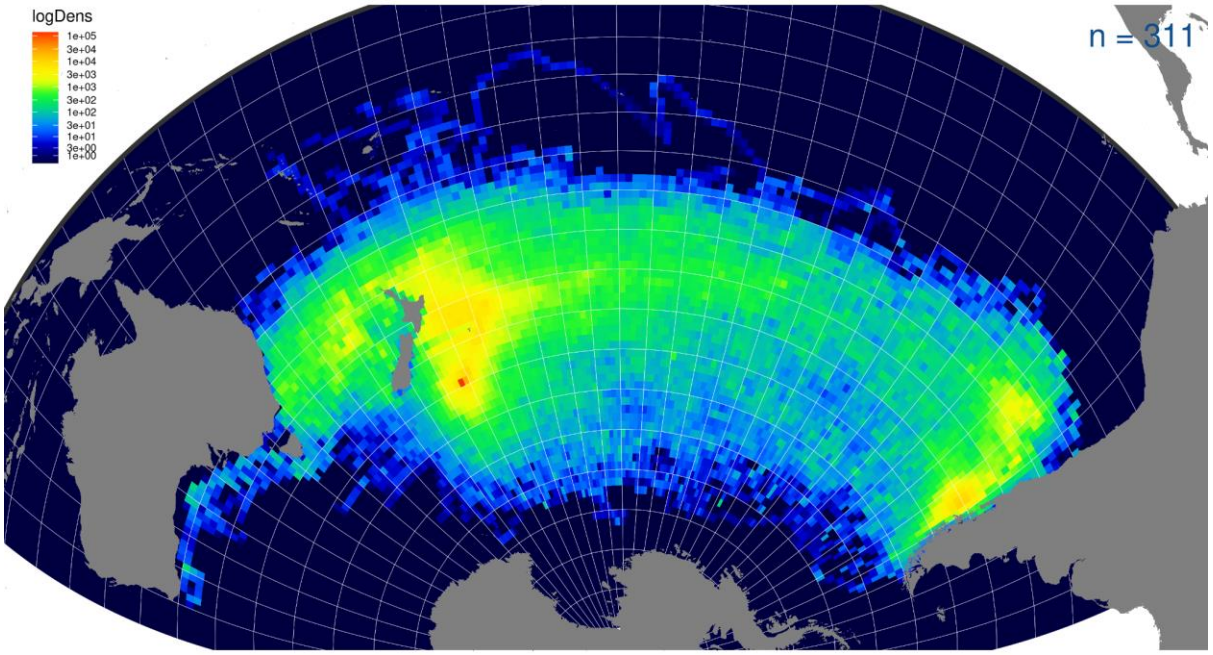

Figure 2: Density (in log-scale) of interpolated tag records for all years and tracked individuals combined, at the 1-degree resolution. The number of tracks is shown in the top-left corner.

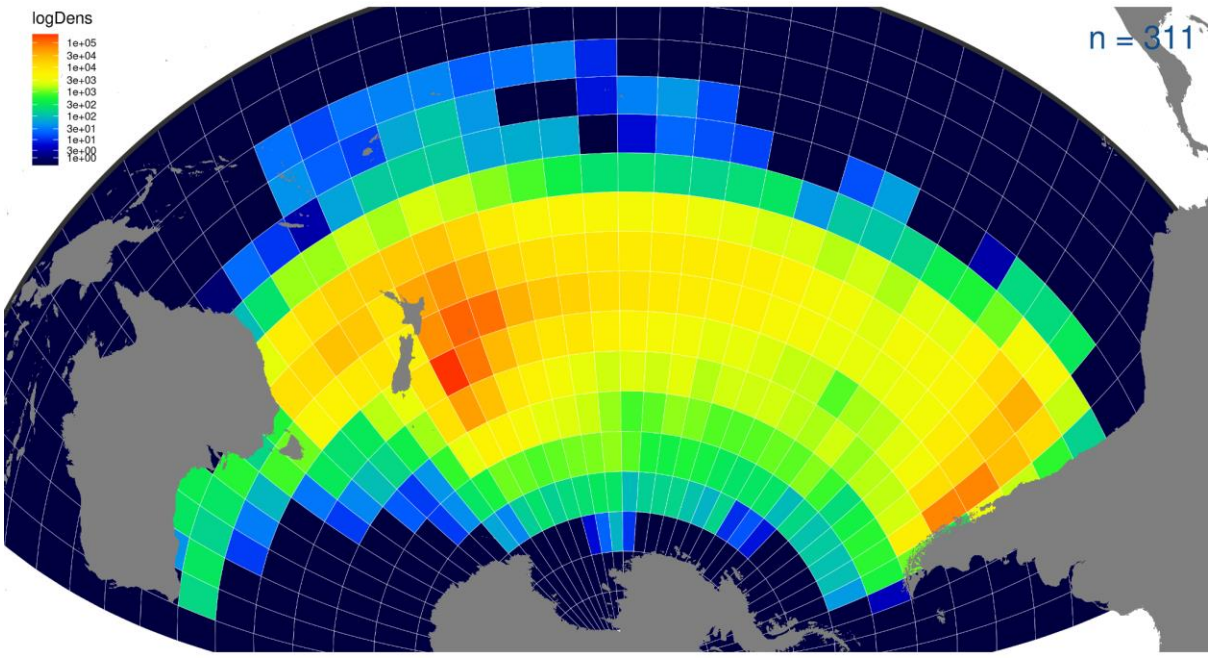

Figure 3: Density (in log-scale) of interpolated tag records for all years and tracked individuals combined, at the 5-degree resolution. The number of tracks is shown in the top-left corner.

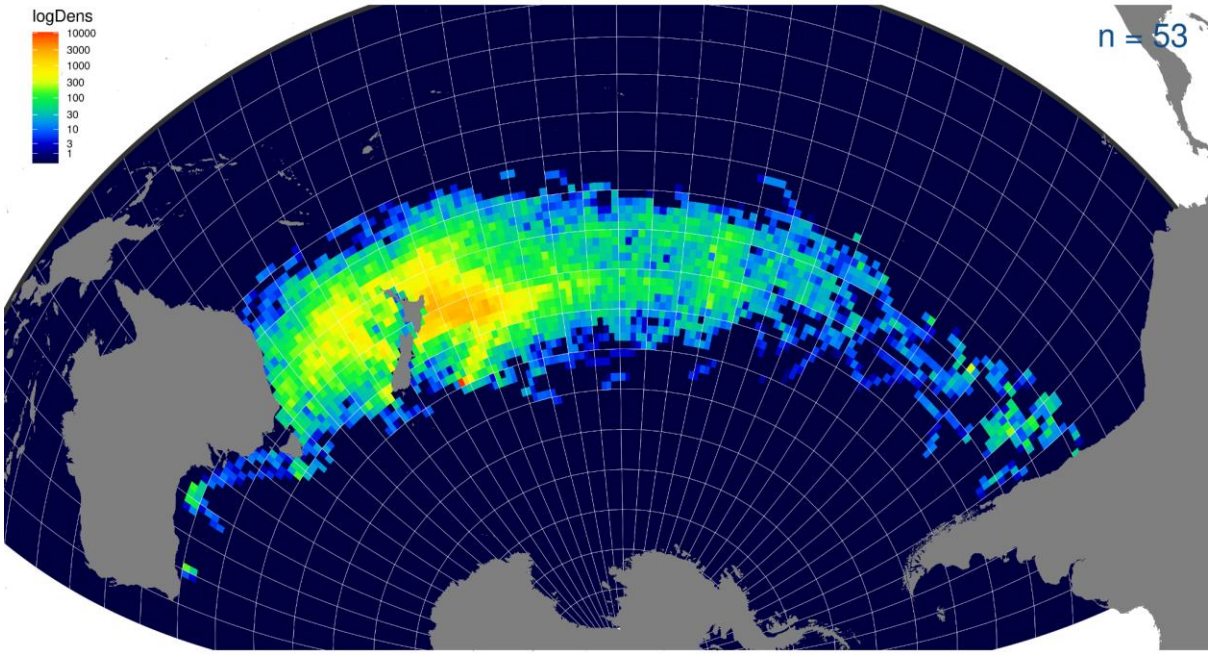

Figure 4: Density (in log-scale) of interpolated tag records for juveniles for all years combined, at the 1-degree resolution. The number of tracks is shown in the top-left corner.

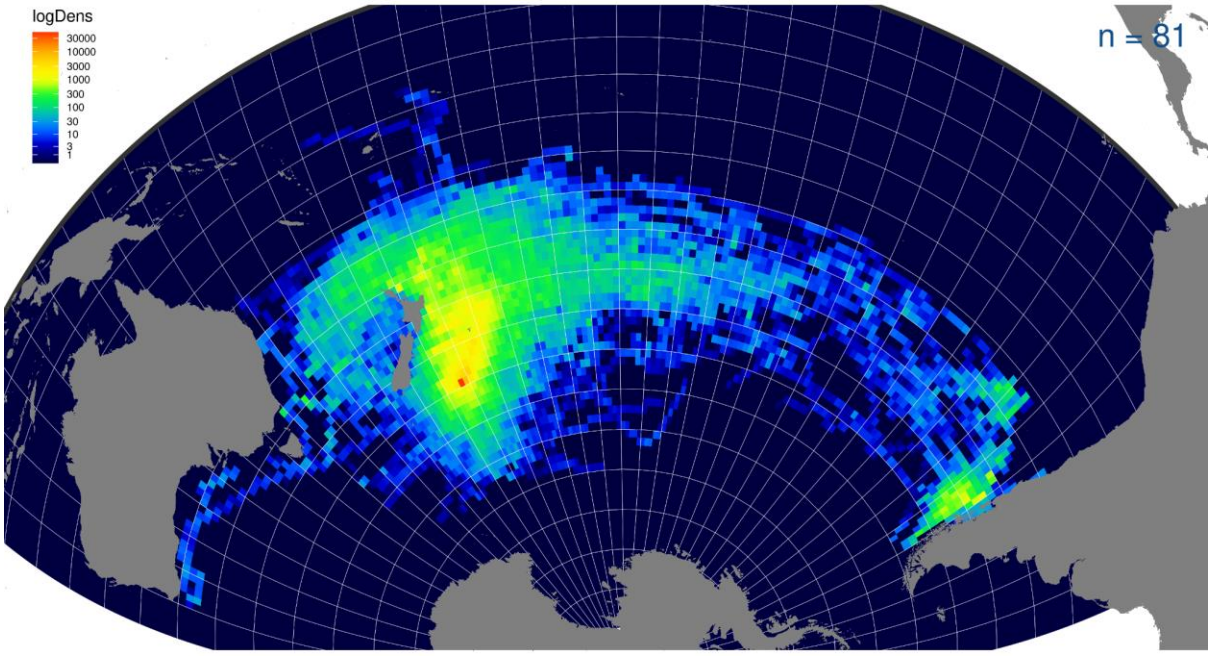

Figure 5: Density (in log-scale) of interpolated tag records for female breeders for all years combined, at the 1-degree resolution. The number of tracks is shown in the top-left corner.

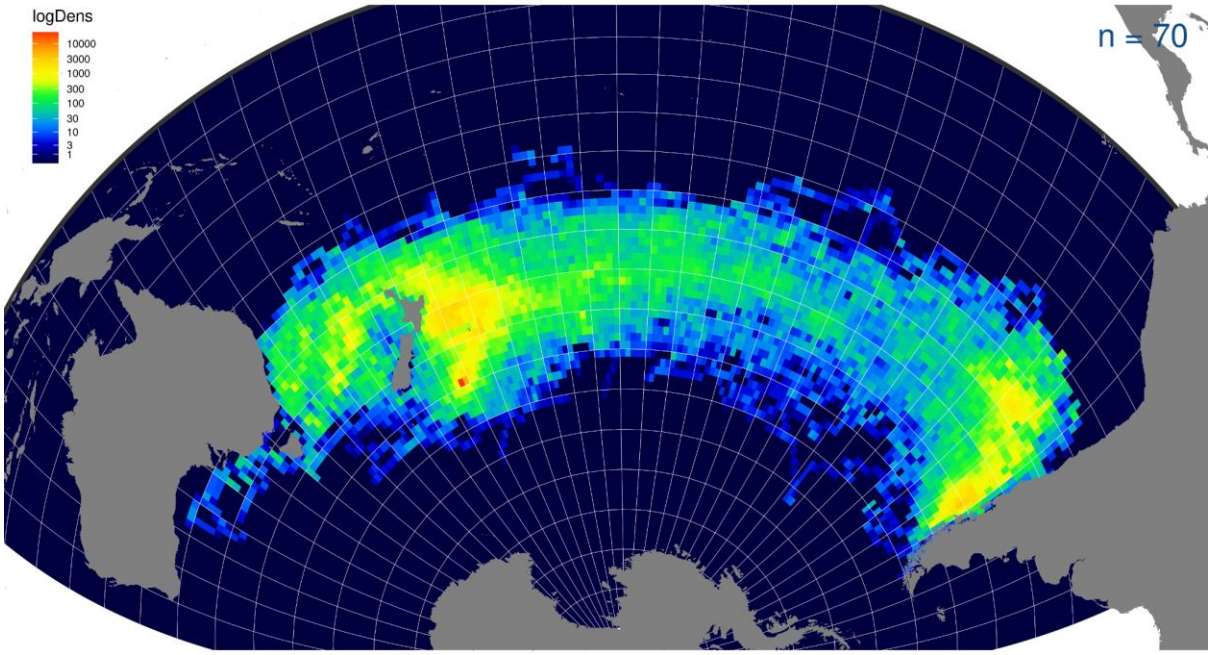

Figure 6: Density (in log-scale) of interpolated tag records for female non-breeders for all years combined, at the 1-degree resolution. The number of tracks is shown in the top-left corner.

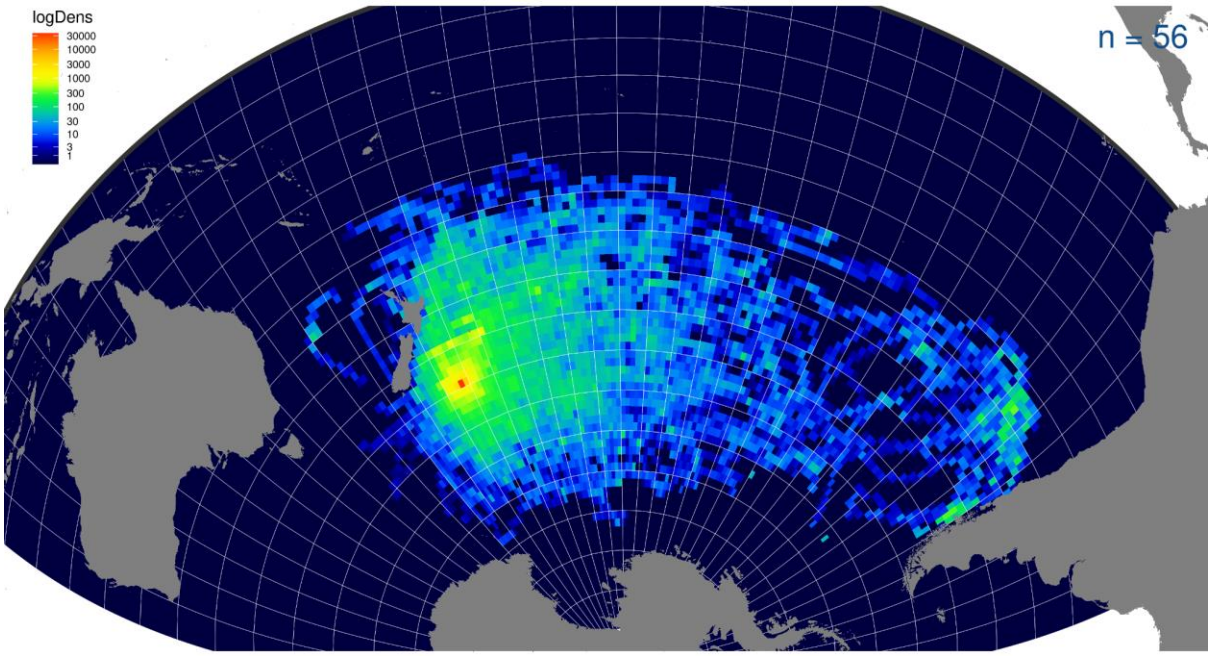

Figure 7: Density (in log-scale) of interpolated tag records for male breeders for all years combined, at the 1-degree resolution. The number of tracks is shown in the top-left corner.

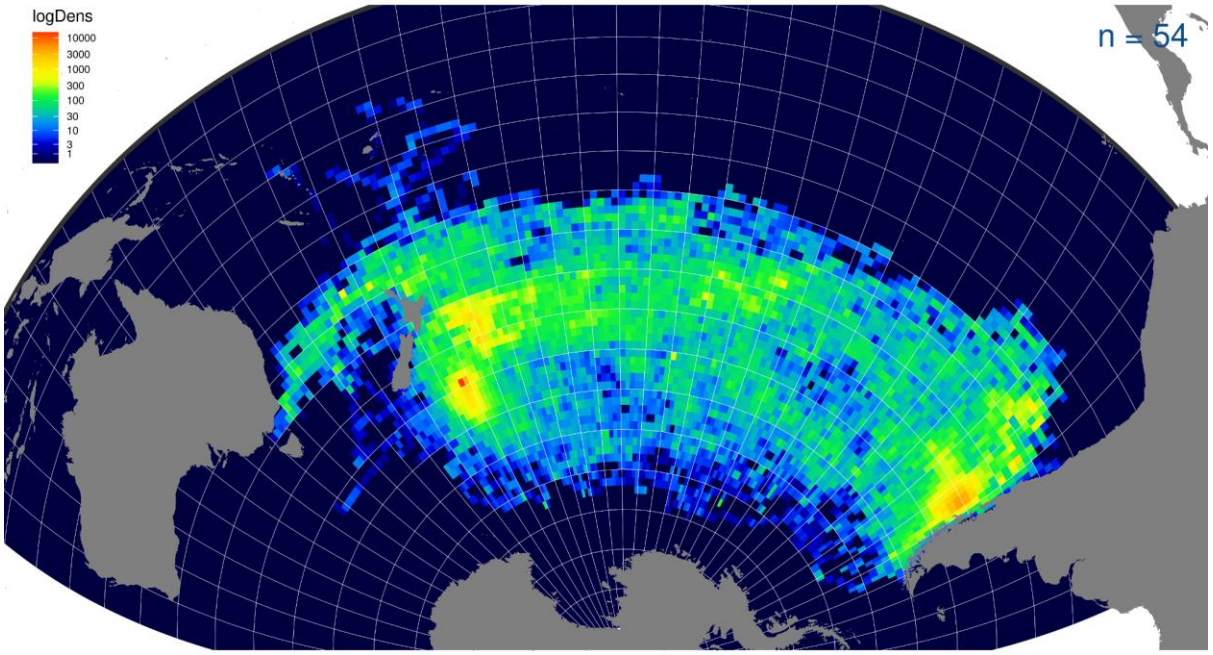

Figure 8: Density (in log-scale) of interpolated tag records for male non-breeders for all years combined, at the 1-degree resolution. The number of tracks is shown in the top-left corner.

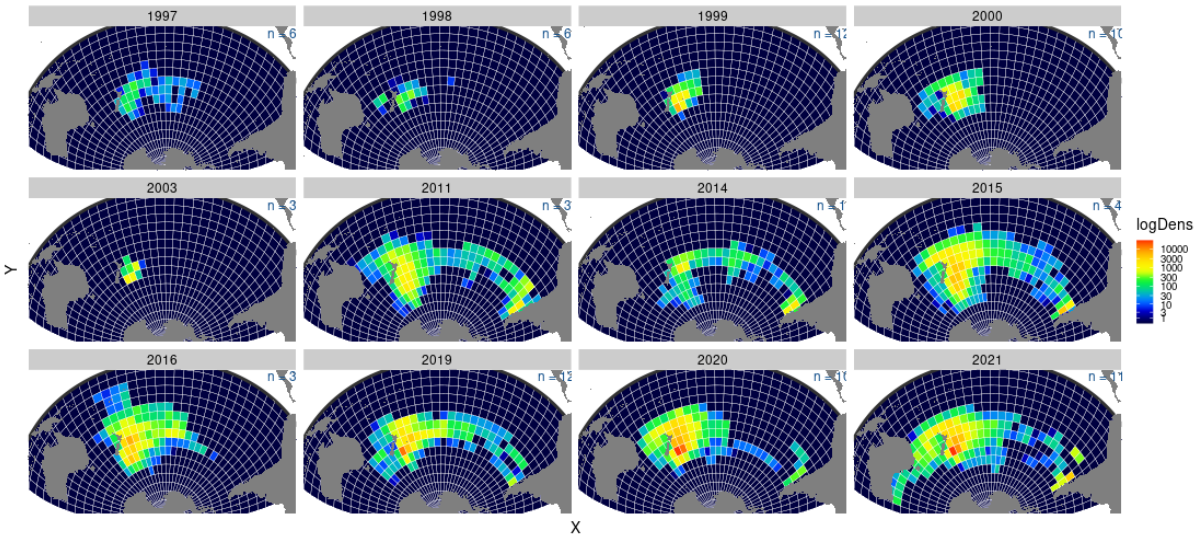

Figure 9: Density (in log-scale) of interpolated tag records for female breeders by observation year, at the 5-degree resolution. The number of tracks by year is shown in the top-left corner of each panel.

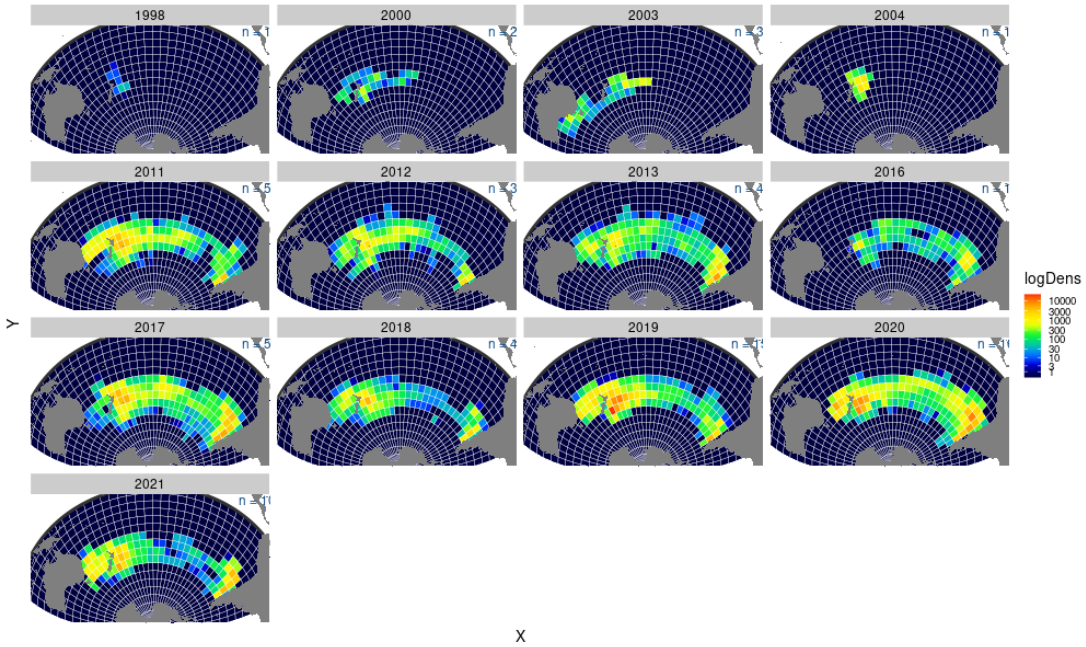

Figure 10: Density (in log-scale) of interpolated tag records for female non-breeders by observation year, at the 5-degree resolution. The number of tracks by year is shown in the top-left corner of each panel.

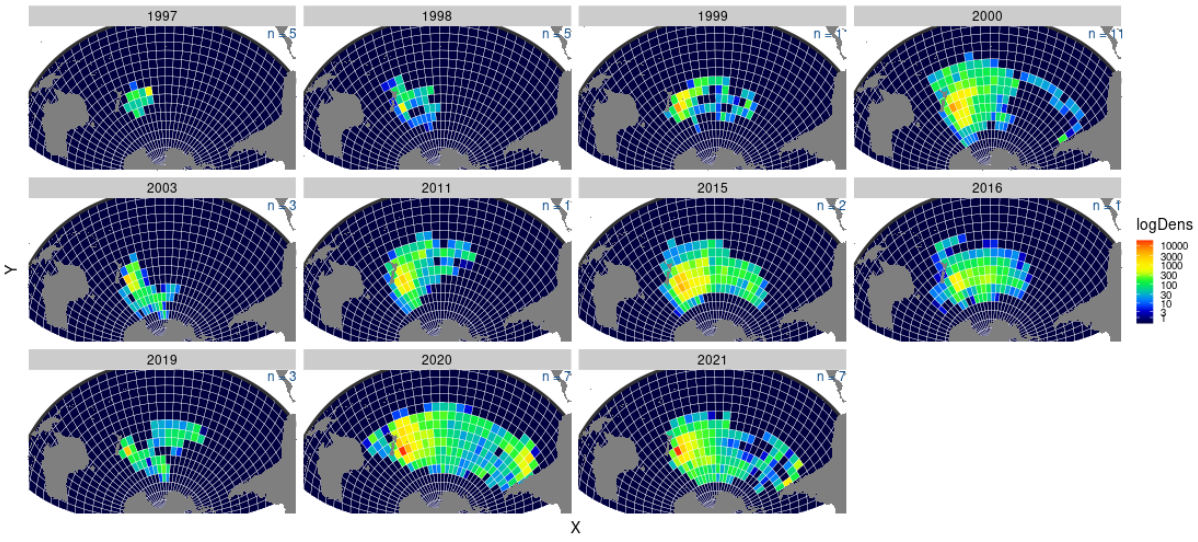

Figure 11: Density (in log-scale) of interpolated tag records for male breeders by observation year, at the 5-degree resolution. The number of tracks by year is shown in the top-left corner of each panel.

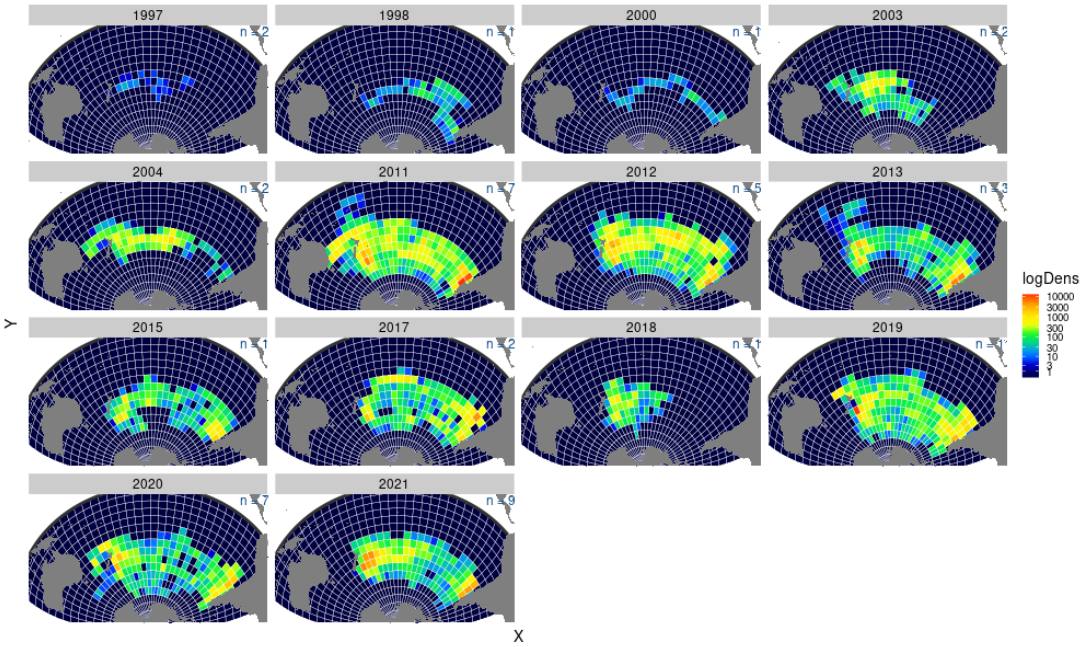

Figure 12: Density (in log-scale) of interpolated tag records for male non-breeders by observation year, at the 5-degree resolution. The number of tracks by year is shown in the top-left corner of each panel.

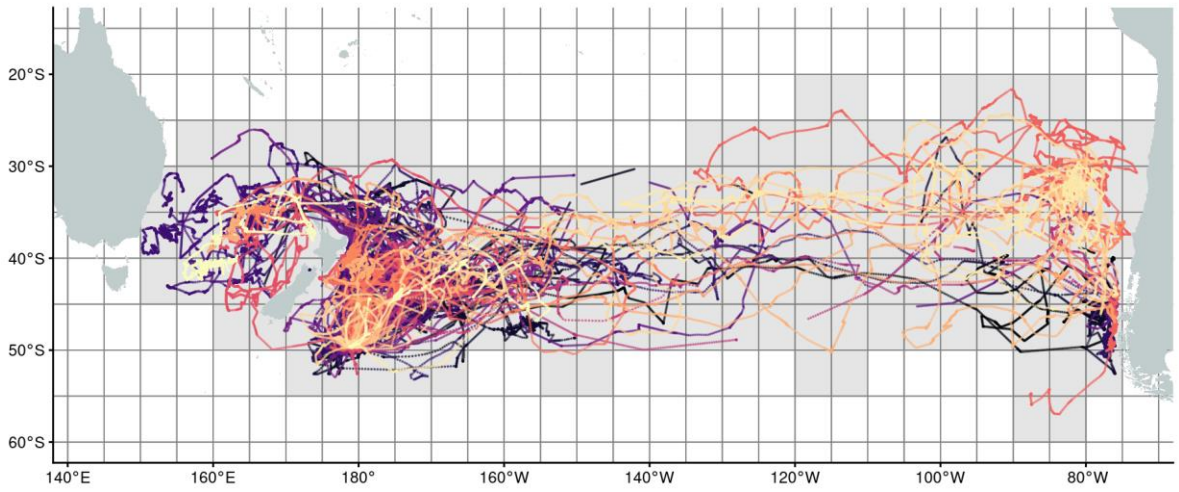

Figure 13: Individual GPS-collected tracks (n=25) for female non-breeders used for the proposed resampling approach. Each track is shown in a different colour. The 5-degree grid used to estimate the distribution is outlined, with the cells included based on the track information filled in grey.

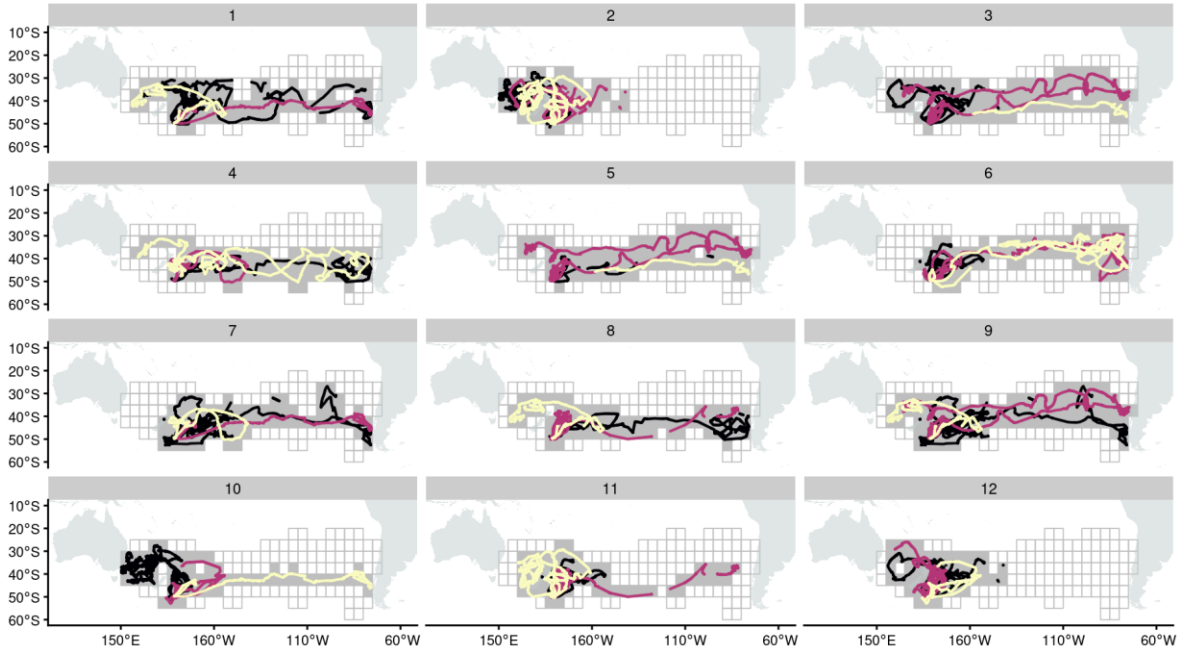

Figure 14: An example of 12 random draws of three tracks from the full set of 25 female non-breeder GPS tracks. The grid cells show the distribution from the full set of tracks, and are filled in grey when they are included as part of the distribution for the current draw of three tracks.

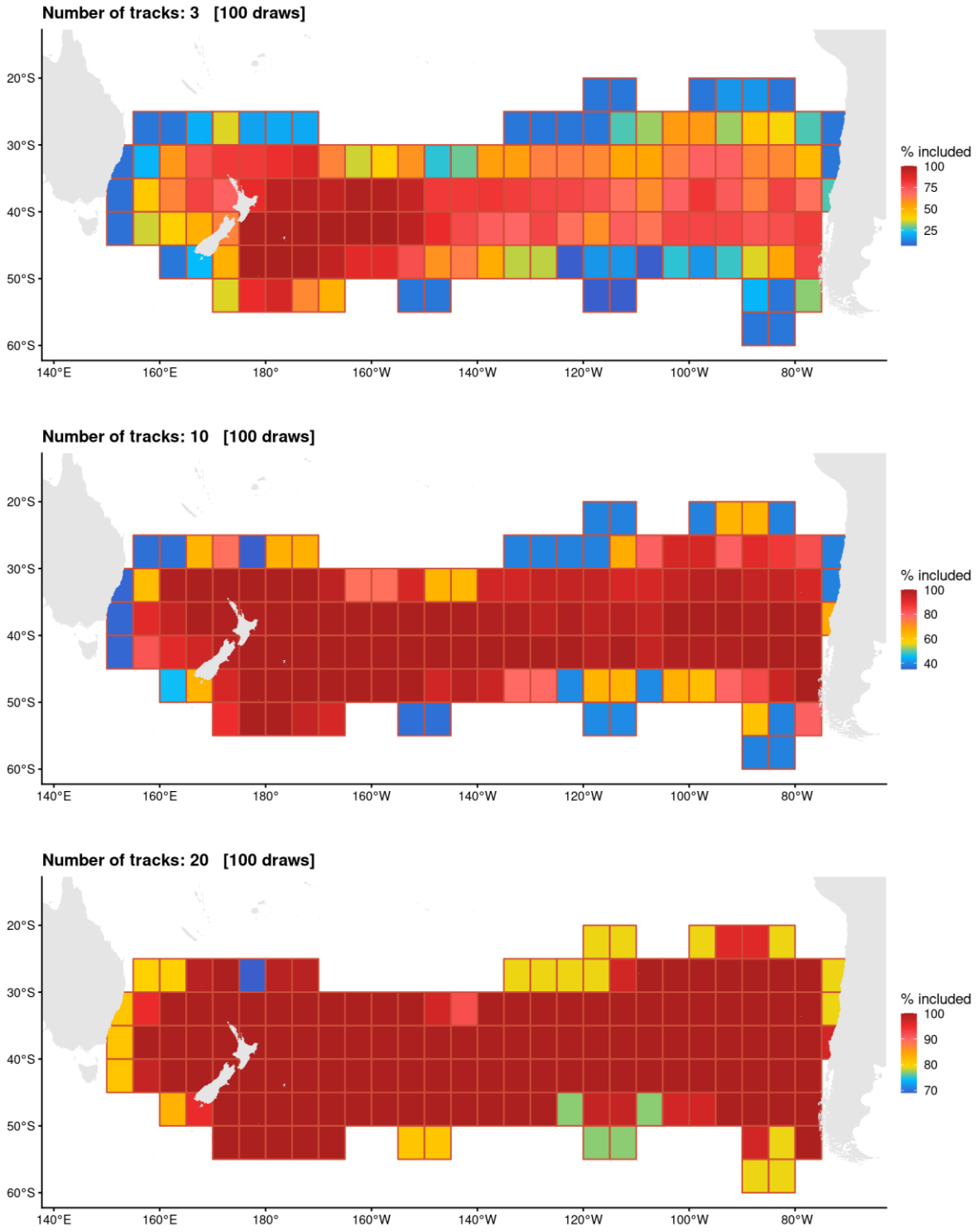

Figure 15: Probability of cell inclusion in the estimated distribution based on the number of tracks used to generate the distribution.

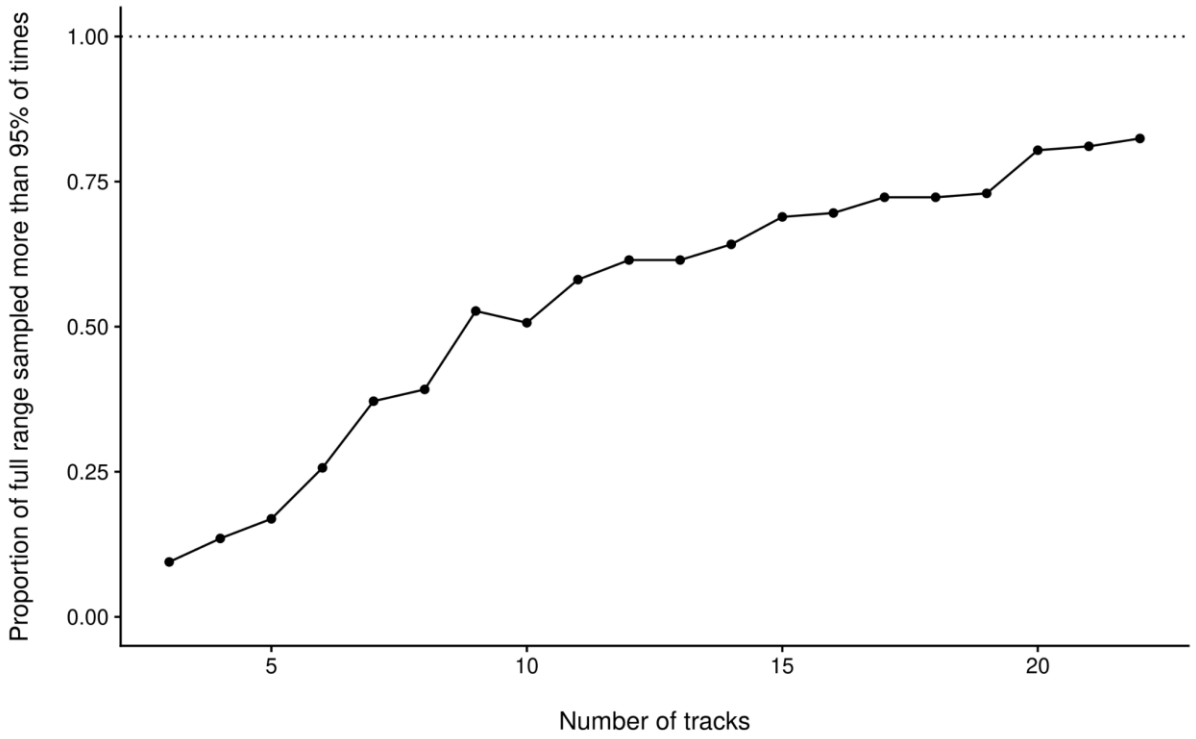

Figure 16: Proportion of the 'full' distribution (as estimated using all 25 female non-breeders GPS tracks) estimated based on the number of tracks included in the sample. Cells are considered as part of the distribution when they were included in at least 95% of resamples.